Coordination of gene expression with cell size enables Escherichia coli to efficiently maintain motility across conditions

Coordination of gene expression with cell size enables *Escherichia coli* to efficiently maintain motility across conditions

Tomoya Honda[1,2*], Jonas Cremer[3,4*], Leonardo Mancini[5,6], Zhongge Zhang[1], Teuta Pilizota[5] and Terence Hwa[1,3§]

[1]Division of Biological Sciences, University of California at San Diego, La Jolla, CA 92093, USA
[2]US Department of Energy, Joint Genome Institute, Berkeley, California 94720, USA
[3]Department of Physics, University of California at San Diego, La Jolla, CA 92093, USA
[4]Department of Biology, Stanford University, Stanford, CA 94305
[5]School of Biological Sciences, Centre for Synthetic and Systems Biology, University of Edinburgh, Edinburgh, UK
[6]Department of Physics, Cavendish Laboratory, University of Cambridge, Cambridge, UK

[*]These authors contributed equally to this work.
[§]correspondence: hwa@ucsd.edu

To swim and navigate, motile bacteria synthesize a complex motility machinery involving flagella, motors, and a sensory system. A myriad of studies has elucidated the molecular processes involved, but less is known about the coordination of motility expression with cellular physiology: In *Escherichia coli*, motility genes are strongly upregulated in nutrient-poor conditions compared to nutrient-replete conditions; yet a quantitative link to cellular motility has not been developed. Here, we systematically investigate gene expression, swimming behavior, cell growth, and available proteomics data across a broad spectrum of exponential growth conditions. Our results suggest that cells up-regulate the expression of motility genes at slow growth to compensate for reduction in cell size, such that the number of flagella per cell is maintained across conditions. The observed 4-5 flagella per cell is the minimum number needed to keep the majority of cells motile. This simple regulatory objective allows *E. coli* cells to remain motile across a broad range of growth conditions, while keeping the biosynthetic and energetic demands to establish and drive the motility machinery at the minimum needed. Given the strong reduction in flagella synthesis resulting from cell size increases at fast growth, our findings also provide a different physiological perspective on bacterial cell size control: A larger cell size at fast growth is an efficient strategy to increase the allocation of cellular resources to the synthesis of those proteins required for biomass synthesis and growth, while maintaining processes such as motility which are only needed on a per-cell basis.

Significance

To swim, bacteria must regulate a battery of motility genes in proper relation to other genes and the environments they encounter. To reveal how cells resolve this challenge, we here study the regulation of motility genes in the model organism *Escherichia coli* across growth conditions. By connecting gene expression with swimming behavior and growth, we illustrate how cells coordinate the regulation of swimming machinery with cell size such that the number of flagella per cell is maintained across conditions. The findings revise previous interpretations which saw swimming motility as a starvation response. Instead, cells are motile across growth conditions with the size-dependent regulation, ensuring an efficient allocation of cellular resources to the synthesis of costly flagella machinery.

Main Text

To thrive in different environments, bacteria must efficiently allocate their limited resources towards different cellular processes in accordance to what is most needed for their growth and survival (1). Flagella driven motility is one of the most distinct processes of bacterial life which provides cells with novel ways to respond to the conditions they encounter (2). The active movement towards more favorable conditions and away from detrimental ones has been studied in detail on the molecular level (3–5) and can give rise to strong fitness advantages (6–9). But flagella driven motility is also a resource demanding process. For growing *E.coli* cells, the synthesis of the motility proteins alone ties up a substantial portion of the protein synthesis resources (10, 11), and the assembly and rotation of flagella also demand energy (12–14). Accordingly, motility expression constitutes a burden on cell growth, such that cells with attenuated motility can grow up to 20 % faster and reach about 10 % higher biomass yields (15–17), a strong difference readily affecting the outcome of (laboratory) evolution (18–21). Given this burden, the expression of motility is expected to be highly controlled, in coordination with other cellular processes and demands (22–25).

Notably, the expression of motility genes varies strongly with the nutrient conditions cells encounter and more resources are allocated to motility expression in nutrient poor than in replete conditions (26–30). These observations have been taken as support for the idea that motility is a response expressed to search for alternative nutrient sources when local nutrient sources are

depleted (26, 29, 30). However, swimming speeds observed during balanced growth do not vary much with the growth rate or the carbon source provided (9). Furthermore, bacterial populations exhibit a chemotaxis-driven form of range expansion (6, 8, 31–33) with expansion speeds which are markedly faster in nutrient replete conditions providing faster growth (9). These latter observations suggest that motility is a phenotype broadly expressed by growing cells, rather than merely being a foraging response to starvation. But why then are motility genes expressed higher in poor growth conditions and how does their degree of expression affect swimming? To resolve this puzzle, we systematically investigated the link between gene expression and swimming in different balanced growth conditions. We found that *E. coli* K-12 cells coordinate their gene expression with cell-size to maintain motility; the upregulation of motility genes at slower growth is a necessary compensation to adjust for growth-related changes in cell size such that the number of flagella per cell remains constant. This simple regulatory objective provides an example of how cells can maintain a function while keeping resource demands minimal. Our findings also provide a new perspective on the relation between cell size control and proteome resource allocation, giving a physiological rationale for the ubiquitously observed positive relation between cell growth and cell size.

To study the relation between swimming behavior and motility gene expression, we first examined gene expression during balanced growth across a broad range of growth conditions, using a physiologically well-characterized strain (WT strain *E. coli* K-12 HE204, **SI Text 1.1**). Motility genes are hierarchically regulated and have been assigned into three different classes with the master regulator *flhDC* being the class-I genes as illustrated in **Fig. S1A** (22–24). We first studied the expression of *fliA*, a class-II gene that encodes the sigma factor σ_F required for the expression of flagella components (class-III genes). Using a LacZ reporter (strain HE207), we quantified the expression level of the *fliA* promoter (in unit of LacZ activity per biomass; see **SI Text 1.4**) during balanced growth, with a range of growth rates obtained by supplementing minimal medium with different carbon sources or rich media components (detailed growth conditions described in **SI Text 1.2**). Consistent with previous reports (26, 28–30), *fliA* expression was higher at slower growth rates (**Fig. 1A**, circles): Expression levels change approximately exponentially with growth rate (dashed line), with a ~4.4 fold increase when growth rates change from fast (1.60 $1/h$ for growth on rich defined medium with glucose) to slow (0.28 $1/h$ for growth on aspartate). The

same trend is observed for the abundance of FliA and other class-II proteins, including the hook-basal body components, as supported by available proteomics data (11) (**Fig. S1BC**). We next studied the promoter activities of a class-I and a class-III gene using LacZ reporters. Expression of the master regulator gene *flhD* (class-I) and the flagellin-encoding gene *fliC* (class-III) also showed similar changes to the *fliA* promoter activity (class-II) (**Fig. S1DE**). The fold change is distinct from a constitutively active promoter, P*tet-lacZ,* which shows significantly less variation in the activity (**Fig. S2AD**). We also verified that the replacement of the native 5'-UTR in *flhD* with the synthetic *lacZ* UTR results in a significantly reduced fold change of *flhD* expression (**Fig. S2BD),** capturing the importance of post-transcriptional regulation (34, 35). In summary, these data suggest that cells express motility genes in a growth-dependent manner and the master regulator *flhDC* plays a key regulatory role for the overall expression.

The observed growth-dependent expression provides a substantial growth-rate dependent burden for the cell. Particularly, a deletion of the master regulator *flhD*, which results in the complete suppression of motility gene expression, increased growth rate by up to 18% compared to the WT strain, with larger increases realized in slower growth conditions where motility expression in the WT is higher (**Fig. S2E**). To rationalize this costly expression and understand its relation to the motile phenotypes, we next characterized the swimming behavior in different growth conditions. Extending a previous approach combining phase contrast microscopy and tracking (9), we quantified the movement of hundreds of cells and analyzed the distributions of observed swimming speeds $\{v_i\}$ during run events (see **Fig. 1B, Fig. S3** and **SI Text 1.3** for methods). We then extracted the average swimming speed and the fraction of *motile cells* with swimming velocities $v_i > 5\ \mu m/s$. Notably, despite the ~4.4 fold change of gene expression (**Fig. 1A**), swimming characteristics varied only weakly: the fraction of swimming cells (α_m) remained close to 90 % for all growth conditions (**Fig. 1C**), and the average swimming speed, $\underline{v} = \langle v_i \rangle$, changed only ~1.3 fold from fast (rich defined medium with glucose) to slow growth (aspartate) (**Fig. 1D**).

One possible explanation for this combined observation of the minor changes in swimming behavior and the large changes in expression of motility genes would be an adjustment to a possible decrease in flagella motor activity at slow growth: The *E. coli* flagella motor is driven by the proton motive force (PMF) and the motor rotation frequency is proportional to the PMF (12, 13). Given

that the PMF is a result of the metabolic state which might change with growth condition, the cell might compensate for slower rotation in poor growth conditions by increasing the expression level of motility genes. To probe this idea, we measured the motor activity by tracking the rotation of beads attached to flagella filaments (36, 37). However, the rotation frequency is found to be almost independent of growth (**Fig. 1E**; a drop of 13 % from growth rate 0.87 $1/h$ to 0.39 $1/h$).

Why then are motility genes expressed more in slow growth conditions? To investigate this question further, we next performed experiments with a synthetic construct which allows for the smooth titration of motility gene expression in a given growth condition, so that we can separately assess the effect of changing motility expression and growth. We replaced the native promoter of the master regulator *flhDC* by the P*tet* promoter, enabling an inducer-dependent control. Additionally, the construct also carries the above-mentioned P*fliA-lacZ* as a reporter for a class-II gene expression (see **Fig. 2A** and **SI Text 1.1.3** for cartoon and details). We first grew this strain in fructose minimal medium with different concentrations of the inducer chlortetracycline (cTc). P*fliA-lacZ* expression decreased smoothly from wild-type levels towards zero when reducing the inducer concentration in the media (**Fig. 2A** blue points). Decreasing the inducer concentration similarly shifted the distribution of swimming speeds (**Fig. 2B)** towards lower average swimming speeds and motile fractions (**Fig. 2CD,** blue points**)**. Similar results were obtained by growing cells in other carbon sources that provide faster and slower growth rates (**Fig. 2,** glucose and mannose as green and magenta points). Overall, these results show that motility gene expression has a strong influence on cellular swimming behaviors at each growth condition, as can also be seen by directly plotting swimming speed and motility fraction against *fliA* expression (**Fig. S4**).

To better understand how the regulation of motility genes determines swimming behavior, we next compared how the swimming phenotypes changes across growth conditions when motility gene expression remains at a constant level. Using the titratable construct and selected inducer levels, we particularly chose two different expression levels (dotted and dashed line) **Fig. 3A**. Comparing the swimming behavior at these two expression levels, we found a gradual reduction of swimming speed as the growth rate slows down (**Fig. 3BC**). This reduction can be largely accounted for by a reduction of the fraction of motile cells (**Fig. 3D**), while the average swimming speed of motile cells remained within narrow ranges (**Fig. 3B**, grey vertical lines). In summary, these observations

suggest that the upregulation of motility genes at slower growth is necessary to keep the population motile but not to increase the swimming speed of the motile cells.

To better understand the regulation of motility genes and its connection to swimming behavior, we next considered the abundance of motility gene products per cell: Gene expression levels, as those determined via a LacZ reporter, are typically quantified per biomass (*e.g.*, the commonly used "Miller Unit" (38) quantifies LacZ activity per biomass; unit $U/\,ml/\mathrm{OD}_{600}$, with OD_{600} having a constant relation with biomass across growth condition (39); see **SI Text 1.4 & SI Text 2**). Since these expression levels correlate with protein mass per biomass as previously discussed (**Fig. S1**), and biomass itself is proportional to cell volume due to the constancy of biomass density (40, 11), the measurements with the class-II gene reporter P*fliA-lacZ* reflect the *concentration* of class-II gene products (flagella hook & basal body; **Fig. S1, Fig. 4A**, top row). As confirmed by the LacZ reporters (**Figs. 1A, S1DE**) and available proteomics data (11) (**Fig. S1BC**), this concentration is higher when cells grow slower. However, bacterial cells also have different cell sizes at different growth rates. In fact, the average biomass per cell exhibits an approximate exponential dependence on the growth rate (**Fig. 4B**), known as the Schaechter-Maaloe-Kjeldgaard relation (41–43). Accordingly, the average *abundance of class-II gene products per cell* is expected to exhibit less change with growth rate than what is observed for the *concentration* (**Fig. 4A**, bottom row). Confirming this idea, the P*fliA-lacZ* expression per cell (unit: $U\,/cell$), taken as the product of expression per biomass (unit: $U\,/\,ml/OD_{600}$) and the average biomass per cell (unit: $ml\cdot OD_{600}/cell$), is nearly independent of growth rate (**Fig. 4C**, filled red points). Remarkably, the exponential relations observed for cell size (**Fig. 4B**, dashed line) and the expression level per biomass (**Fig. 4C**, dashed black line) show similar absolute rates ($1.18\,h^{-1}$ and $1.17\,h^{-1}$), leading to the abundance per cell being independent of growth rate (**Fig. 4C**, dotted red line).

The above analysis suggests that cells maintain their *number* of flagella across growth conditions and that the large change of gene expression with growth rate is necessary to keep this number constant as the cell size changes. To confirm this idea more directly, we counted the number of flagella filaments attached to the cells using a staining assay (**Fig. S5** and **SI Text 1.5**). We confirmed that the average number of flagella filaments per WT cell remains within a narrow range across growth conditions (4-5, within the measurement error), see **Fig. S5D**. As an example, two

cells of different sizes but similar flagella numbers are shown in **Fig. 4D**. Looking at the distribution of filament numbers across the population, we see that very few cells possess only one or zero filaments (**Fig. S5B**), consistent with a high fraction of motile cells (**Fig. 1C**). In contrast, the average number of filaments varied strongly for the titratable *flhDC* strain as the provided inducer concentration was varied (**Fig. S6**). Particularly, the fraction of cells with zero or one filament clearly increased at lower inducer concentrations (**Fig. S6AB**) which coincides with the increase in the fraction of non-motile cells at lower inducer concentrations (**Fig. 2D**). We further confirmed that the class-II gene reporter expression reflects the change of filament number (**Fig. 4E**): reducing P*fliA-lacZ* level by titrating *flhDC* expression led to a linear drop of the average number of filaments in different growth conditions (**Fig. 4E**, open symbols). In contrast, the WT strain exhibited little variation in either the filament number or gene expression per cell (**Fig. 4E**, filled circles). In combination, these findings support the idea that cells regulate motility genes in coordination with cell size such that an average number of flagella per cell is maintained in different growth conditions.

To see how efficiently the motility genes are regulated, consider the relation between the average number of flagella per cell, and the fraction of motile cells (**Fig. 4F**): When the expression of motility genes is low such that there are on average less than four flagella per cell (*flhDC* titration with low inducer levels, diamonds), the motile fraction is proportional to the average flagella number (**Fig. 4F**, grey region: limited motility). In contrast, when expression levels reach close to those of WT such that there are on average more than four flagella per cell, almost all cells are motile (**Fig. 4F**, circle points and yellow region: full motility). An even higher expression level per cell would only increase the costs to express extra flagella and is not observed (**Fig. 4F**, blue region: non-efficient expression). *E. coli* K-12 thus appears to regulate its motility expression levels such that the associated resource demands to synthesize and rotate flagella are at the minimum necessary to keep most cells motile. While the requirement for on average 4 flagella per cell ensures most cells to be motile (yellow region in **Fig. 4F**), this number is also close to what is minimally required to allow uninterrupted motility when cells half the number of their flagella during cell division.

Discussion

In this study, we analyzed the regulation of motility genes by *E. coli* in different balanced growth conditions. We found that the fold-change in gene expression per biomass compensates for the variation in cell size, resulting in the average number of flagella per cell remaining constant across growth conditions. This simple regulatory scheme ensures a fully motile population while keeping resource demands to synthesize and rotate flagella to a minimum.

How do cells implement this regulation scheme? Future studies are needed to reveal further mechanistic insights, but our results pinpoint to the combined roles of transcriptional and post-transcriptional regulation in determining the abundance of the motility master regulator FlhDC. On the transcriptional level, cAMP-CRP dependent activation on *flhDC* expression (44, 45) may play an important role, as other cAMP-CRP dependent genes are known to increase with decreasing growth rates under carbon limitation (27, 46). In addition, the post-transcriptional regulation on *flhDC* expression might further be essential, as we find that the modification of the 5'-UTR strongly affects *flhDC* expression. In this context, it is tempting to speculate about the physiological roles of sRNA species which are increasingly discovered and found to be involved in diverse regulatory tasks (47, 48). Further, post-translational regulation on *flhD* via the anti-FlhDC factor (YdiV) might be involved in adjusting the expression of *fliA* and other class-II motility genes such that their expression scales with cell size (25).

The findings reported here have implications for bacterial motility from the ecological perspective, particularly concerning its role in promoting fitness across different environments. Previous works have highlighted the upregulation as a fingerprint of anticipatory response with motility triggered when nutrients run out (26, 28–30). In contrast, we here propose that at least a part of the upregulation of swimming in poorer growth conditions is not a starvation response *per se* but an obligatory regulation to maintain sufficiently high flagella numbers and swimming as cell size changes. Future studies are needed to investigate how our findings merge with the ideas of anticipatory response, but the efficient regulation of motility genes to maintain swimming under growth-supporting conditions is in line with the observations that bacterial cells quickly stop swimming (9), actively brake motor rotation (49, 50), and even release their flagella upon entering starvation (51, 52). Notably, the maintenance of cellular motility in growth-supporting conditions

enables cell population to rapidly expand into unoccupied nutrient rich territories, boosting overall population growth (9). The growth advantage of such a navigated range expansion relies on cells being motile across conditions, and a delayed onset of motility only in response to starvation would nullify the fitness advantage (9). Therefore, the efficient regulation of motility genes described here does not only minimize the resources required to build and fuel the motility machinery, but it also supports fast navigated range expansion which further boost fitness (9, 21, 33).

The findings further provide a new perspective on the relation between cell-size and growth itself. Throughout the text, we have referred to the change in motility gene expression as an up-regulation in poor nutrient conditions. But this change can also be viewed as a down-regulation in nutrient replete conditions when cells grow fast. Given that the goal of the flagella regulatory system is to maintain the number of flagella per cell, we can view the decreased flagella expression at fast growth also as a consequence of increased cell size at fast growth. This view leads us to suggest a physiological rationale for *E. coli*'s choice of cell size at different growth rates. It is generally preferrable for bacterial cells to keep a small biomass (i.e., cell size) as it promotes efficient diffusive transport, fast nutrient uptake, and strong dispersal (53, 54). However, in favorable conditions allowing for rapid growth, the translational machinery per biomass is the most growth-limiting factor (55, 56) and making cell-size larger can be beneficial to alleviate this bottleneck: By increasing its size at fast growth, the cell effectively reduces the amount of flagella proteins that need to be synthesized, thus allowing more proteomic resources to be allocated towards ribosomes and other components of the translation machinery. Quantitatively, flagella proteins comprise ~3.0 % of the total protein mass in slow carbon-limited conditions and ~0.7 % in rich-defined medium (11). Thus, by increasing its cell size, *E. coli* manages to "save" 2.3 % of the proteome that would have otherwise been tied up in flagella synthesis. To put this amount in perspective, the entire set of biosynthesis enzymes saved when cells are provided with all amino acids and nucleotides is only ~11 % of the proteome (comparing the proteome composition of cells grown in rich-defined medium supplemented with glucose to those grown in glucose minimal medium). This saving accounts for a large share of the increase of growth rate from 1.0 $1/h$ in glucose minimal medium to 1.8 $1/h$ in rich-defined medium (11), based on the well-established linear relation between the ribosome content and growth rate, where every percent-of-proteome added to the protein synthesis machinery results in an ~0.06 $1/h$ increase in growth rate (11, 27,

55). Thus a 2.3 % saving in proteome allocation to flagella synthesis would amount to a gain of ~0.14 $1/h$ for growth in rich medium. In other words, had *E. coli* kept its size at that in poor nutrient condition, then it would suffer a 0.14 $1/h$ reduction in growth rate (from the observed growth rate of 1.8 $1/h$) in rich medium just due to motility expression alone. This proteome resource savings by a change of cell size should be similarly applicable to other cellular processes which demand protein expression on a per-cell basis, including cell division and cell pole maintenance. Therefore, increasing cell size at fast growth might be a simple and effective strategy to reduce competition for proteome resources at fast growth, for *E. coli* and possibly many other fast growing bacterial species.

Materials and Methods

Strains used in this study

The reference strain in our study is a motile variant of the *E. coli* K-12 (strain NCM3722B) whose physiology has been well-characterized in previous studies (17, 27, 46, 57, 58). Similar to other motile K-12 strains (59, 60), the strain NCM3722B carries a 1 kb insertion element (IS*1*) upstream of *flhDC* transcription site that activates *flhDC* expression and the motile phenotype (44, 61). Detailed information on the strain and derived constructs to report gene expression levels and titrate *flhDC* expression are provided in **SI Text 1.1**.

Growth media

Cells were grown in a modified MOPS-buffered minimal medium (62). Trace micronutrients were not added as the metal components have been reported to inhibit motility (63). To change growth conditions, different carbon sources were provided. When indicated, casamino acids (CAA) and rich defined medium (RDM) were additionally provided. When titrating *flhDC* expression, cTc was provided as an inducer. For the swimming assay and the flagella staining, 0.05 % PVP40 was provided to prevent cells and flagella from sticking to material surfaces (64). Additional details on the media composition and concentrations are provided in **SI Text 1.2.1**.

Strain culturing and growth rate measurement

Growth measurements were performed in a 37 °C water bath shaker operating at 250 rpm. Each growth experiment was carried out in three steps: seed culture in LB broth, pre-culture, and experimental culture in identical minimal medium. In the seed culture, a single fresh colony from a LB agar plate was inoculated into liquid LB broth and cultured at 37 °C for 4–5 h. Cells were then cultured in the specified medium at 37 °C overnight (pre-culture). The starting OD_{600} in pre-culture was adjusted so that exponential cell growth was maintained. After the pre-culturing, cells were then diluted to OD_{600} = 0.005–0.02 in identical pre-warmed medium and grown in a 37 °C water bath shaker (experimental culture). After cells had been grown at least for three generations, OD_{600} was measured around every half doubling of cell growth. About 4–6 data points below OD_{600} 0.3 were used to calculate growth rate. For the cell culturing in rich conditions using CAA and RDM,

the experimental cultures were started by diluting saturated precultures and repeating growth and dilution to restore steady state growth. The cultures were then diluted into fresh medium to start the measurements. Additional details are provided in **SI Text 1.2.2**.

Measurements of swimming characteristics

To quantify the swimming behavior of cells, samples of 200 µl cell culture were collected at different time points during steady state growth. Immediately after the collection, samples were diluted to an OD_{600} of approximately 0.005 using filtered growth medium. The diluted sample was then loaded into a rectangular capillary and a phase-contrast microscopy was used to acquire the videos of the swimming cells. A custom-made Python script was then used to obtain cell trajectories and swimming characteristics. Additional details of the experiments and data analysis are provided in **SI Text 1.3**. The code is available via GitHub at https://github.com/jonascremer/swimming_analysis.

β-galactosidase assay

Samples were collected at different time points during steady state growth and β-galactosidase activity was measured by a traditional Miller method. LacZ expression level was determined by taking a linear regression of LacZ activity against OD_{600}. Additional details are provided in **SI Text 1.4**.

Flagella number and length quantification

Flagella staining was performed by using strains that carry S219C modification in *fliC* sequence. This allows a direct labeling of flagella filaments by sulfhydryl-specific Alexa Fluor maleimide dyes (65–67). Cell samples were collected around at OD_{600} 0.2 during steady state in each condition. Following the washing step, flagella filaments were labeled by the Alexa Fluor 488 Maleimide dye under a dark condition at 37 °C for 15 min. After washing out the excess dye, cells were imaged between a glass cover and 2 % agar pad using a confocal microscope (Leica LSM 8). Fluorophores were excited with a 488 nm laser line and the detectors scanned in the wave-length range 500−550 nm. Images of 60-100 cells were acquired for each experiment. The number of flagella was counted manually, and the length equivalent was determined by dividing the integrated fluorescent

signals by the number of flagella for each cell. Additional details of the experiments and data analysis are provided in **SI Text 1.5**.

Motor speed measurement

A strain carrying sticky-*fliC* was used for the experiment. Cells were collected during steady state growth and the flagella were sheared using two syringes connected by a plastic tube. Following the shearing steps, cells were loaded into a flow cell and exposed to a suspension of beads with diameter 0.5 μm. The motor speed was measured via back-focal plane interferometry to track bead rotations (68). Full details of the experiments and data analysis are provided in **SI Text 1.6**.

Acknowledgement

We thank Matteo Mori, Chenhao Wu, and Christina Ludwig for providing proteomic data, and Angela Dawson and Ekaterina Krasnopeeva for providing the pTOF24 plasmids carrying S219C and sticky *fliC*. Tomoya Honda acknowledges the JASSO long-term graduate fellowship and JSPS overseas research fellowship. Leonardo Mancini and Teuta Pilizota acknowledge the support of the Cunningham Trust award ACC/KWF/PhD1. Work in the Hwa lab is supported by the NIH through grant R01GM109069 and by the NSF through grant MCB 1818384.

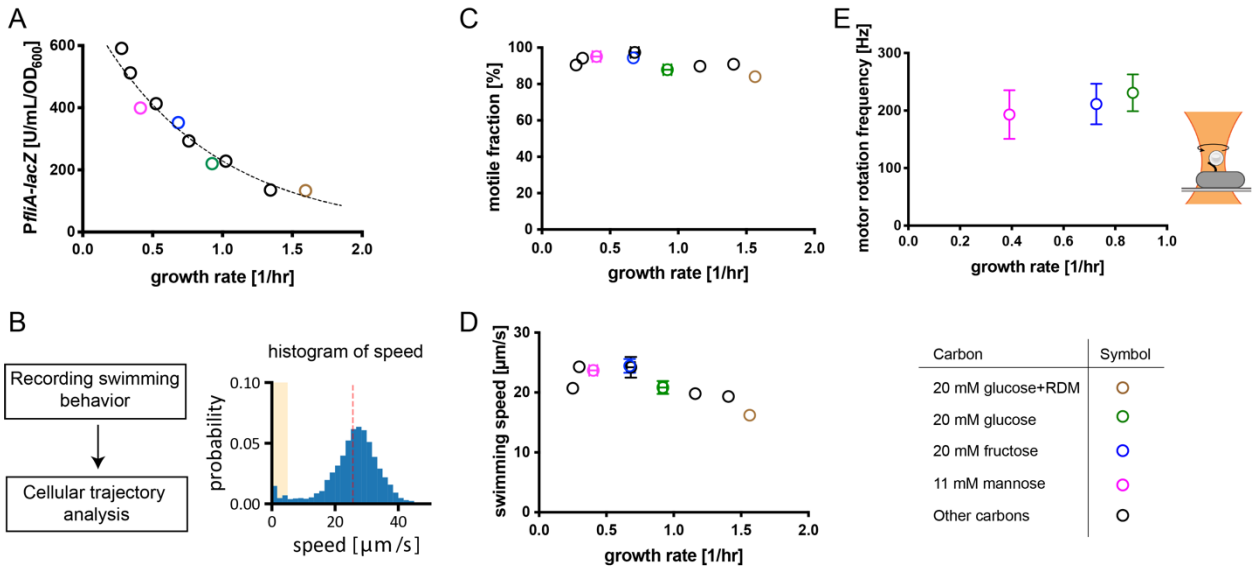

Fig. 1: Motility gene expression and swimming behavior during balanced growth in different growth media. (A) Expression level of a reporter of the *fliA* promoter (a class-II gene; Fig. S1A) for growth on different carbon sources (circles). The reporter expression changes strongly with growth rates. Dashed line indicates exponential fit, $734 \cdot e^{-k \cdot \lambda}$ with rate $k = 1.17\ 1/h$. **(B)** Quantification of swimming behavior: Using a phase contrast microscopy, cells were tracked and swimming speeds were analyzed (details in **SI Text 1.3**). Cell-to-cell variation of swimming speeds for growth on fructose as example. The red line indicates the mean swimming speed, and the yellow background indicates the range defined as non-motile (swimming speeds $v_i < 5\ \mu m/s$). Additional conditions and reproducibility are shown in **Fig. S3**. **(C, D)** Motile fractions and average swimming speeds for different growth rates, which show minor variations with growth-rate. Error bars of s.d. are provided when biological replicates are available (**Table S6 & Fig. S3**). **(E)** Motor rotation frequency for different growth rates. Error bars indicate s.d. observed for the probed population (**Table S7**). Rotation frequencies of beads attached to filament stub were measured using back-focal plane interferometry and a strain with the filament gene modified to readily stick to polystyrene beads (sticky-*fliC*) (68, 69), see cartoon and **SI Text 1.6**. Data in rich media were not collected because rapid cell divisions prevented the motor observation for sufficient periods. Four reference conditions are highlighted by colors as indicated in the legend table. Strains HE207, HE206 and HE608 were used in (A), (C,D) and (E), respectively. The data values are listed in **Table S2 and S6-7**.

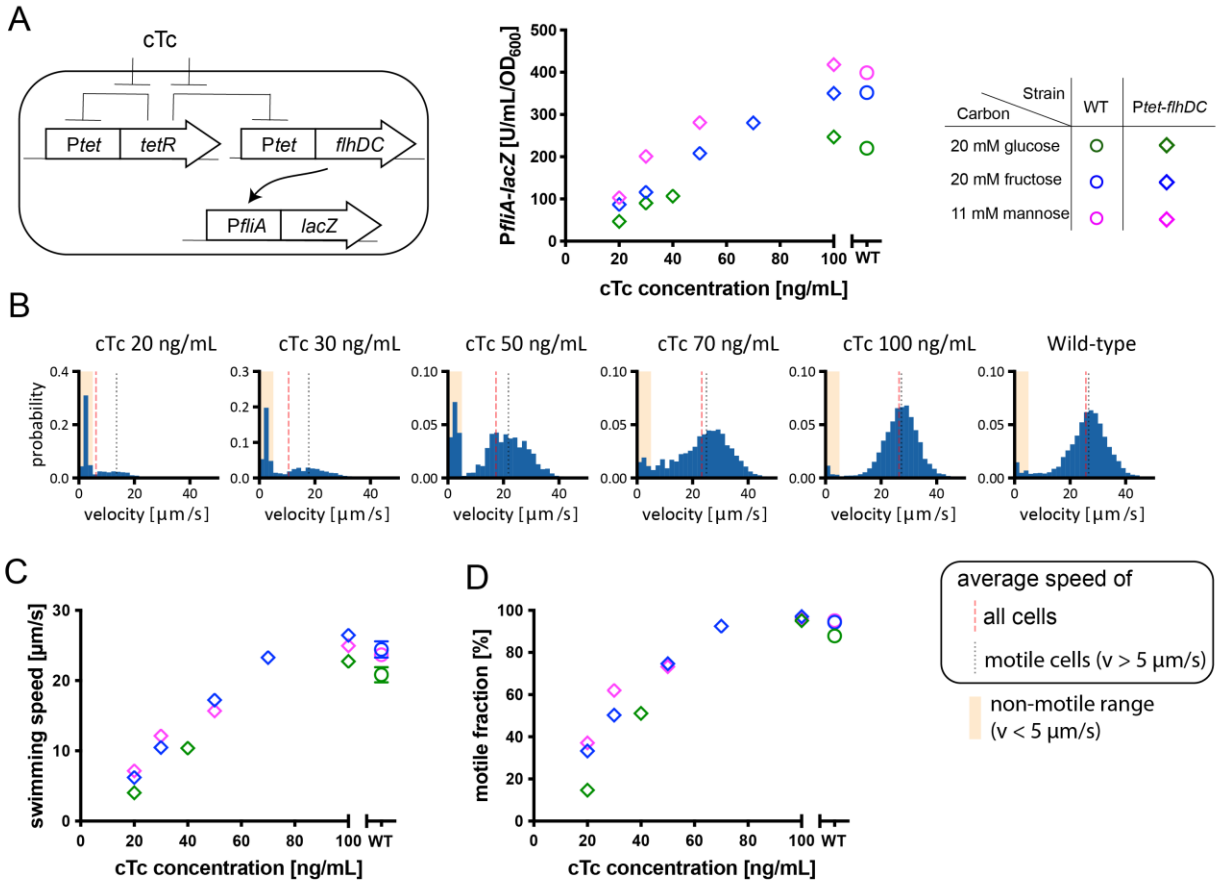

Fig. 2: Gene expression and swimming behavior when titrating a motility master regulator. (A) Titratable *flhDC* construct with P*fliA-lacZ* reporter to quantify *fliA* expression. Titration control is achieved via the P*tet* system and cTc as inducer. P*fliA-lacZ* expression was measured by varying inducer concentration. (**B**) Swimming speed distributions when cells are grown on fructose with different inducer levels. (**C** & **D**) Changes in average swimming speed and the motile fraction of cells (swimming speed > 5 µm/s) in the population. WT are shown as circles in A, C, D for comparison. Strains HE641 and HE170 were used in (A) and (B, C, D), respectively (both strains are identical except carrying different *lacZ* reporters: **Table S1**). The data values are listed in **Table S8-9**.

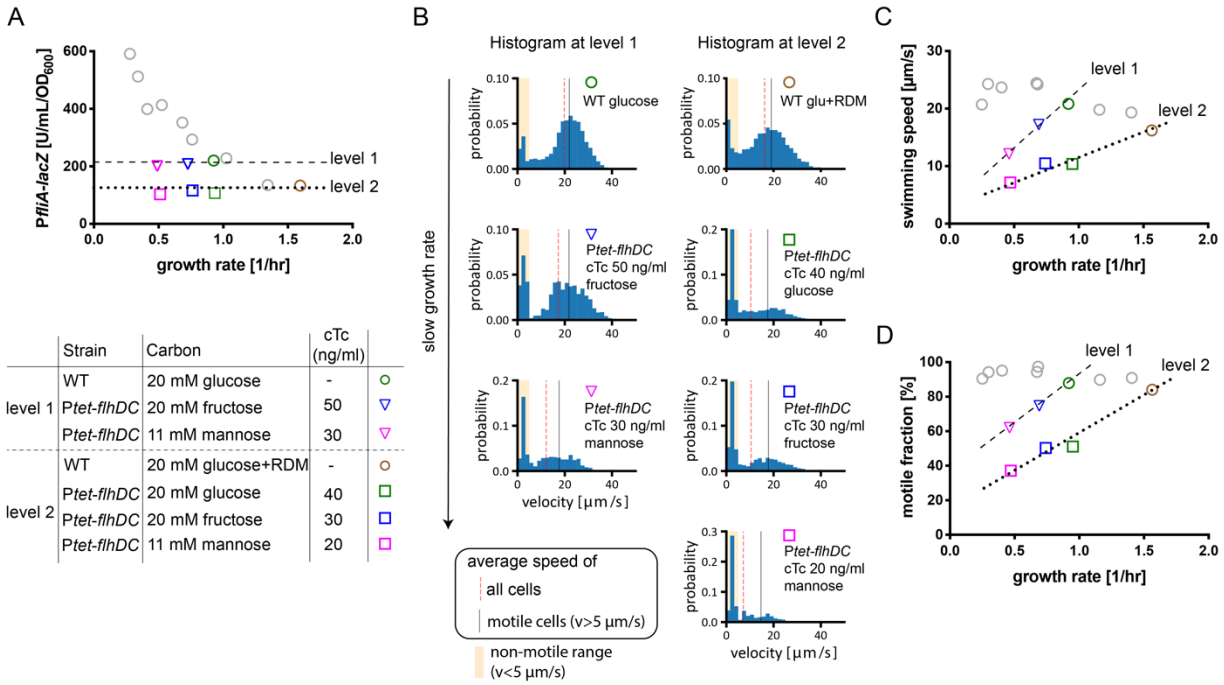

	Strain	Carbon	cTc (ng/ml)	
level 1	WT	20 mM glucose	-	○
	Ptet-flhDC	20 mM fructose	50	▽
	Ptet-flhDC	11 mM mannose	30	▽
level 2	WT	20 mM glucose+RDM	-	○
	Ptet-flhDC	20 mM glucose	40	□
	Ptet-flhDC	20 mM fructose	30	□
	Ptet-flhDC	11 mM mannose	20	□

Fig. 3: Swimming behavior across growth conditions at fixed motility expression. (**A**) P*fliA-lacZ* expression against growth rate when the expression levels are set independent of growth rate by using the titratable *flhDC* construct. To obtain the indicated expression levels, inducer (cTc) concentrations for each growth condition were selected based on the data in Fig. 2A and listed in the legend table. One expression level (level 1, dashed line) resembles the level observed for WT cells growing on glucose (green circle), and the other (level 2, dotted line) resembles the level for WT cells growing on glucose+RDM (rich defined medium) (brown circle). The other data of P*fliA-lacZ* expression in WT are shown as grey circles for comparison (same data as Fig.1A). (**B**) Distributions of swimming speed for the two expression levels (left column: level 1, right column: level 2). The fraction of non-motile cells increases for decreasing growth rate (bars in yellow regions), while the swimming speed of motile cells ($v_i > 5\ \mu m/s$) barely changes (grey lines). The reduction of average swimming with decreasing growth rate (red dot lines) is thus largely accounted for by the increase of non-motile fraction. **(C, D)**. The average swimming speed (C) and motile fraction (D) drop for the two fixed expression levels as growth rates decrease (dashed and dotted lines), while WT cells (grey circles, same data as Fig.1 CD) exhibit minor changes. Strain HE641 and HE170 were used in (A) and (B, C, D), respectively.

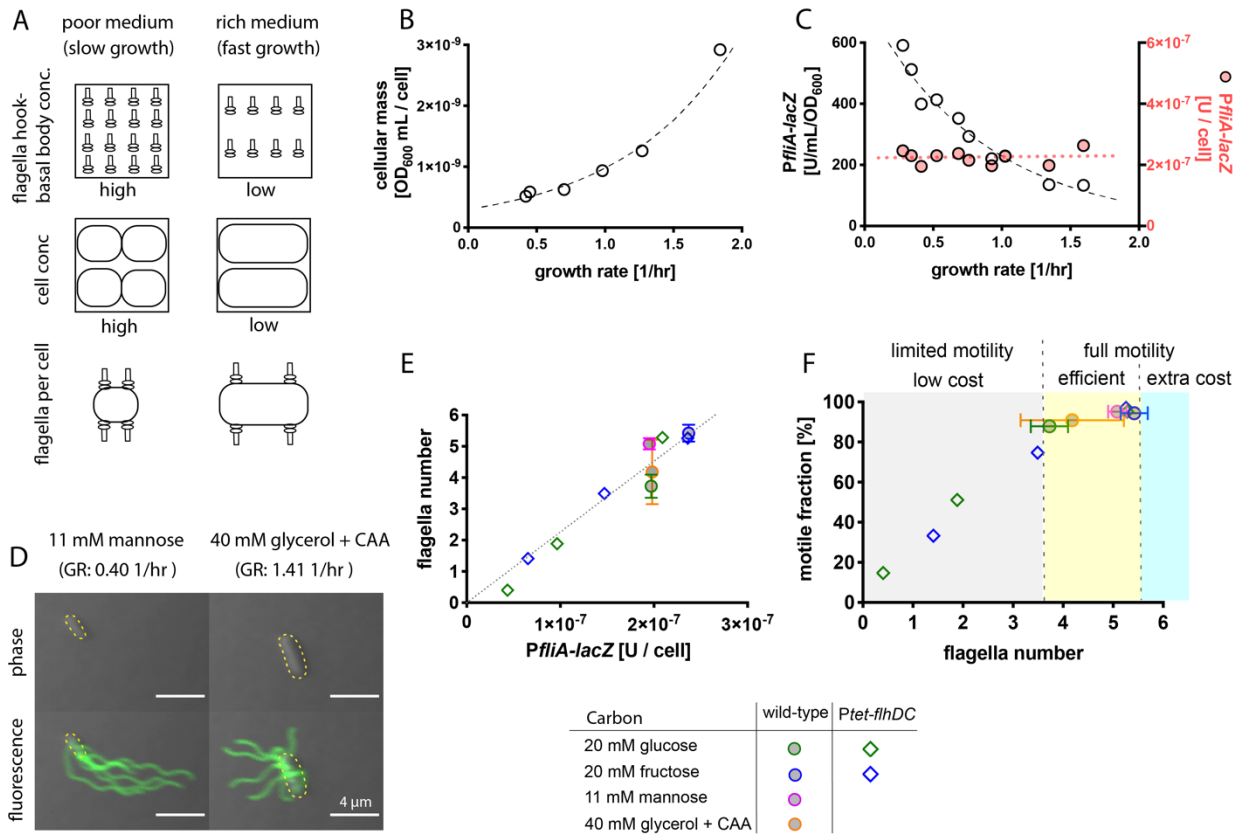

Fig. 4: Expression levels change with cell size such that cells remain motile across growth conditions. (A) The concentration of motility gene products per unit biomass is higher for growth in poor condition (top), but cells are also smaller when growing slower (middle). Consequently, the abundance of motility gene products expressed per cell, like the number of flagella, would show less variation across growth conditions (bottom). **(B)** The average biomass of cells, determined via optical density measurements and cell counting (CFU in culture), increases exponentially with growth rate. Line indicates exponential fit, $\sim e^{k \cdot \lambda}$, with growth rate λ and parameter $k = 1.18\ 1/h$. **(C)** Expression of the class-II gene *fliA* per biomass (open circles) and per cell (red circles) based on the P*fliA-lacZ* measurements (strain HE207). Dashed line shows an exponential fit for the P*fliA-lacZ* expression per biomass, $\sim e^{k \cdot \lambda}$ with rate $k = -1.17\ 1/h$. A red dotted line indicates the product of the two exponential relations in cell size (B) and P*fliA-lacZ* per biomass. **(D)** Images of cells with stained flagella filaments in a poor and rich condition (slow and fast growth, left and right column). While cell size differs (phase contrast, top row), a similar number of flagella filaments is observed (fluorescently labeled filaments, bottom row). Full

distribution across the population shown in Fig. S5. Yellow lines indicate cell perimeter. **(E)** Relation between flagella filament number and P*fliA-lacZ* expression per cell for the native (filled circles) and titratable (diamonds) regulation of *flhDC* expression. Line indicates a linear fit with slope $2.26 \cdot 10^7$. Different inducer levels were used for the titratable *flhDC* strain as shown in Fig. S6. **(F)** Motile fraction and flagella number for wild-type (circles) and titratable *flhDC* strain (diamonds). WT cells are mostly motile and adjust their expression level per cell to ensure motility (yellow region) while preventing more expression than needed (blue region). Strains HE206 and HE170 were used to obtain swimming data. Strains HE207 and HE641 were used to obtain P*fliA-lacZ* expression data. Flagella filament numbers were quantified using strains HE582 and HE571 harboring a modified S219C *fliC* sequence. Cell size data in (B) from Basan *et al* (39). Data values are listed in **Table S10-11**.

References

1. D. Molenaar, R. van Berlo, D. de Ridder, B. Teusink, Shifts in growth strategies reflect tradeoffs in cellular economics. *Molecular Systems Biology* **5**, 323 (2009).

2. H. C. Berg, *E. coli in Motion* (Springer-Verlag, 2004) https:/doi.org/10.1007/b97370 (April 19, 2021).

3. U. Alon, M. G. Surette, N. Barkai, S. Leibler, Robustness in bacterial chemotaxis. *Nature* **397**, 168–171 (1999).

4. V. Sourjik, N. S. Wingreen, Responding to chemical gradients: bacterial chemotaxis. *Curr Opin Cell Biol* **24**, 262 268 (2012).

5. A. J. Waite, N. W. Frankel, T. Emonet, Behavioral Variability and Phenotypic Diversity in Bacterial Chemotaxis. *Annual Review of Biophysics* **47**, 595–616 (2018).

6. J. Adler, Chemotaxis in bacteria. *Science* **153**, 708 716 (1966).

7. I. Chet, R. Mitchell, Ecological Aspects of Microbial Chemotactic Behavior. *Annual Review of Microbiology* **30**, 221–239 (1976).

8. D. A. Koster, A. Mayo, A. Bren, U. Alon, Surface Growth of a Motile Bacterial Population Resembles Growth in a Chemostat. *Journal of Molecular Biology* **424**, 180–191 (2012).

9. J. Cremer, *et al.*, Chemotaxis as a navigation strategy to boost range expansion. *Nature* **575**, 658–663 (2019).

10. D. W. Erickson, *et al.*, A global resource allocation strategy governs growth transition kinetics of Escherichia coli. *Nature* **551**, 119 123 (2017).

11. M. Mori, *et al.*, From coarse to fine: the absolute Escherichia coli proteome under diverse growth conditions. *Molecular Systems Biology* **17**, e9536 (2021).

12. D. C. Fung, H. C. Berg, Powering the flagellar motor of Escherichia coli with an external voltage source. *Nature* **375**, 809–812 (1995).

13. C. V. Gabel, H. C. Berg, The speed of the flagellar rotary motor of Escherichia coli varies linearly with protonmotive force. *PNAS* **100**, 8748–8751 (2003).

14. T. Minamino, Protein export through the bacterial flagellar type III export pathway. *Biochimica et Biophysica Acta (BBA) - Molecular Cell Research* **1843**, 1642–1648 (2014).

15. E. J. Gauger, *et al.*, Role of Motility and the flhDC Operon in Escherichia coli MG1655 Colonization of the Mouse Intestine. *Infection and Immunity* **75**, 3315–3324 (2007).

16. X. Wang, T. K. Wood, IS 5 inserts upstream of the master motility operon flhDC in a quasi-Lamarckian way. *The ISME Journal* **5**, 1517–1525 (2011).

17. M. Basan, *et al.*, Overflow metabolism in Escherichia coli results from efficient proteome allocation. *Nature* **528**, 99 104 (2015).

18. X. Yi, A. M. Dean, Phenotypic plasticity as an adaptation to a functional trade-off. *eLife* **5**, e19307 (2016).

19. D. T. Fraebel, *et al.*, Environment determines evolutionary trajectory in a constrained phenotypic space. *Elife* **6**, e24669 (2017).

20. B. Ni, *et al.*, Evolutionary Remodeling of Bacterial Motility Checkpoint Control. - PubMed - NCBI. *Cell Reports* **18**, 866 877 (2017).

21. W. Liu, J. Cremer, D. Li, T. Hwa, C. Liu, An evolutionarily stable strategy to colonize spatially extended habitats. *Nature* **575**, 664–668 (2019).

22. G. S. Chilcott, K. T. Hughes, Coupling of Flagellar Gene Expression to Flagellar Assembly in Salmonella enterica Serovar Typhimurium and Escherichia coli. *Microbiol Mol Biol Rev* **64**, 694–708 (2000).

23. S. Kalir, *et al.*, Ordering Genes in a Flagella Pathway by Analysis of Expression Kinetics from Living Bacteria. *Science* **292**, 2080–2083 (2001).

24. D. M. Fitzgerald, R. P. Bonocora, J. T. Wade, Comprehensive Mapping of the Escherichia coli Flagellar Regulatory Network. *PLOS Genetics* **10**, e1004649 (2014).

25. J. M. Kim, M. Garcia-Alcala, E. Balleza, P. Cluzel, Stochastic transcriptional pulses orchestrate flagellar biosynthesis in Escherichia coli. *Science Advances* **6**, eaax0947 (2020).

26. C. D. Amsler, M. Cho, P. Matsumura, Multiple factors underlying the maximum motility of Escherichia coli as cultures enter post-exponential growth. *Journal Of Bacteriology* **175**, 6238 6244 (1993).

27. S. Hui, *et al.*, Quantitative proteomic analysis reveals a simple strategy of global resource allocation in bacteria. *Mol Syst Biol* **11**, e784–e784 (2015).

28. B. Ni, R. Colin, H. Link, R. G. Endres, V. Sourjik, Growth-rate dependent resource investment in bacterial motile behavior quantitatively follows potential benefit of chemotaxis. *PNAS* **117**, 595–601 (2020).

29. M. Liu, *et al.*, Global Transcriptional Programs Reveal a Carbon Source Foraging Strategy by Escherichia coli. *J Biol Chem* **280**, 15921–15927 (2005).

30. K. Zhao, M. Liu, R. R. Burgess, Adaptation in bacterial flagellar and motility systems: from regulon members to 'foraging'-like behavior in E. coli. *Nucleic Acids Res* **35**, 4441 4452 (2007).

31. J. Saragosti, *et al.*, Directional persistence of chemotactic bacteria in a traveling concentration wave. *PNAS* **108**, 16235–16240 (2011).

32. X. Fu, *et al.*, Spatial self-organization resolves conflicts between individuality and collective migration. *Nature Communications* **9**, 2177 (2018).

33. S. Gude, *et al.*, Bacterial coexistence driven by motility and spatial competition. *Nature* **578**, 588–592 (2020).

34. N. De Lay, S. Gottesman, A complex network of small non-coding RNAs regulate motility in Escherichia coli. *Molecular Microbiology* **86**, 524–538 (2012).

35. E. Levine, Z. Zhang, T. Kuhlman, T. Hwa, Quantitative Characteristics of Gene Regulation by Small RNA. *PLoS Biol* **5**, e229 (2007).

36. W. S. Ryu, R. M. Berry, H. C. Berg, Torque-generating units of the flagellar motor of Escherichia coli have a high duty ratio. *Nature* **403**, 444–447 (2000).

37. E. Krasnopeeva, C.-J. Lo, T. Pilizota, Single-Cell Bacterial Electrophysiology Reveals Mechanisms of Stress-Induced Damage. *Biophysical Journal* **116**, 2390–2399 (2019).

38. J. H. Miller, Experiments in molecular genetics (1972) (May 11, 2021).

39. M. Basan, *et al.*, Inflating bacterial cells by increased protein synthesis. *Mol Syst Biol* **11**, 836–836 (2015).

40. C. L. Woldringh, J. S. Binnerts, A. Mans, Variation in Escherichia coli buoyant density measured in Percoll gradients. *J Bacteriol* **148**, 58–63 (1981).

41. M. Schaechter, O. MaalØe, N. O. Kjeldgaard, Dependency on Medium and Temperature of Cell Size and Chemical Composition during Balanced Growth of Salmonella typhimurium. *Microbiology,* **19**, 592–606 (1958).

42. F. Si, *et al.*, Invariance of Initiation Mass and Predictability of Cell Size in Escherichia coli. *Current Biology* **27**, 1278–1287 (2017).

43. H. Zheng, *et al.*, General quantitative relations linking cell growth and the cell cycle in Escherichia coli. *Nature Microbiology* **5**, 995–1001 (2020).

44. K. A. Fahrner, H. C. Berg, Mutations That Stimulate flhDC Expression in Escherichia coli K-12. *Journal of Bacteriology* **197**, 3087–3096 (2015).

45. O. Soutourina, *et al.*, Multiple Control of Flagellum Biosynthesis in Escherichia coli: Role of H-NS Protein and the Cyclic AMP-Catabolite Activator Protein Complex in Transcription of the flhDC Master Operon. *Journal of Bacteriology* **181**, 7500–7508 (1999).

46. C. You, *et al.*, Coordination of bacterial proteome with metabolism by cyclic AMP signalling. *Nature* **500**, 301–306 (2013).

47. M. K. Mihailovic, *et al.*, High-throughput in vivo mapping of RNA accessible interfaces to identify functional sRNA binding sites. *Nat Commun* **9**, 4084 (2018).

48. F. De Mets, L. Van Melderen, S. Gottesman, Regulation of acetate metabolism and coordination with the TCA cycle via a processed small RNA. *Proceedings of the National Academy of Sciences* **116**, 1043–1052 (2019).

49. A. Boehm, *et al.*, Second Messenger-Mediated Adjustment of Bacterial Swimming Velocity. *Cell* **141**, 107–116 (2010).

50. K. Paul, V. Nieto, W. C. Carlquist, D. F. Blair, R. M. Harshey, The c-di-GMP Binding Protein YcgR Controls Flagellar Motor Direction and Speed to Affect Chemotaxis by a "Backstop Brake" Mechanism. *Molecular Cell* **38**, 128–139 (2010).

51. J. L. Ferreira, *et al.*, γ-proteobacteria eject their polar flagella under nutrient depletion, retaining flagellar motor relic structures. *PLOS Biology* **17**, e3000165 (2019).

52. X.-Y. Zhuang, *et al.*, Live-cell fluorescence imaging reveals dynamic production and loss of bacterial flagella. *Molecular Microbiology* **114**, 279–291 (2020).

53. A. L. Koch, WHAT SIZE SHOULD A BACTERIUM BE? A Question of Scale. *Annu. Rev. Microbiol.* **50**, 317–348 (1996).

54. K. D. Young, The Selective Value of Bacterial Shape. *Microbiol. Mol. Biol. Rev.* **70**, 660–703 (2006).

55. M. Scott, C. W. Gunderson, E. M. Mateescu, Z. Zhang, T. Hwa, Interdependence of Cell Growth and Gene Expression: Origins and Consequences. *Science* **330**, 1099–1102 (2010).

56. M. Scott, S. Klumpp, E. M. Mateescu, T. Hwa, Emergence of robust growth laws from optimal regulation of ribosome synthesis. *Molecular Systems Biology* **10**, 747 (2014).

57. E. Soupene, *et al.*, Physiological Studies of Escherichia coli Strain MG1655: Growth Defects and Apparent Cross-Regulation of Gene Expression. *J Bacteriol* **185**, 5611–5626 (2003).

58. S. D. Brown, S. Jun, Complete Genome Sequence of Escherichia coli NCM3722. *Genome Announc.* **3** (2015).

59. F. R. Blattner, *et al.*, The Complete Genome Sequence of Escherichia coli K-12. *Science* **277**, 1453–1462 (1997).

60. J. S. Parkinson, Complementation analysis and deletion mapping of Escherichia coli mutants defective in chemotaxis. *Journal of Bacteriology* **135**, 45–53 (1978).

61. C. S. Barker, B. M. Prüß, P. Matsumura, Increased Motility of Escherichia coli by Insertion Sequence Element Integration into the Regulatory Region of the flhD Operon. *Journal of Bacteriology* **186**, 7529–7537 (2004).

62. S. Cayley, M. T. Record, B. A. Lewis, Accumulation of 3-(N-morpholino)propanesulfonate by osmotically stressed Escherichia coli K-12. *Journal of Bacteriology* **171**, 3597–3602 (1989).

63. J. ADLER, B. TEMPLETON, The Effect of Environmental Conditions on the Motility of Escherichia coli. *Microbiology,* **46**, 175–184 (1967).

64. H. C. Berg, L. Turner, Chemotaxis of bacteria in glass capillary arrays. Escherichia coli, motility, microchannel plate, and light scattering. *Biophysical Journal* **58**, 919–930 (1990).

65. L. Turner, R. Zhang, N. C. Darnton, H. C. Berg, Visualization of Flagella during Bacterial Swarming. *Journal of Bacteriology* **192**, 3259–3267 (2010).

66. L. Turner, A. S. Stern, H. C. Berg, Growth of Flagellar Filaments of Escherichia coli Is Independent of Filament Length. *Journal of Bacteriology* **194**, 2437–2442 (2012).

67. L. Turner, H. C. Berg, "Labeling Bacterial Flagella with Fluorescent Dyes" in *Bacterial Chemosensing: Methods and Protocols*, Methods in Molecular Biology., M. D. Manson, Ed. (Springer, 2018), pp. 71–76.

68. J. Rosko, V. A. Martinez, W. C. K. Poon, T. Pilizota, Osmotaxis in Escherichia coli through changes in motor speed. *PNAS* **114**, E7969–E7976 (2017).

69. L. Mancini, *et al.*, Escherichia coli's physiology can turn membrane voltage dyes into actuators. *bioRxiv*, 607838 (2019).